JOC Article

# Synthesis, Spectroscopic, Electrochemical and $Pb^{2+}$-Binding Studies of Tetrathiafulvalene Acetylene Derivatives

Yao-Peng Zhao, Li-Zhu Wu,* Gang Si, Yan Liu, Hai Xue, Li-Ping Zhang, and Chen-Ho Tung

*Laboratory of Organic Optoelectronic Functional Materials and Molecular Engineering, Technical Institute of Physics and Chemistry and Graduate University, Chinese Academy of Sciences, Beijing 100080, People's Republic of China*

*lzwu@mail.ipc.ac.cn*

*Received October 31, 2006*

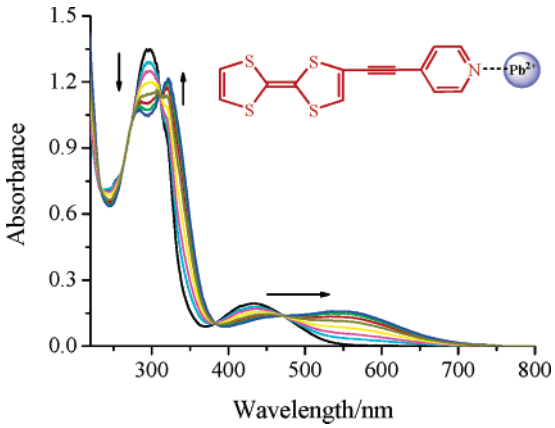


A series of tetrathiafulvalene acetylene derivatives, [TTF−C≡C−A] [A = $C_6H_4N(CH_3)_2$-4 (**1**), $C_6H_4$-$OCH_3$-4 (**2**), $C_6H_5$ (**3**), $C_6H_4F$-4 (**4**), $C_6H_4NO_2$-4 (**5**), $C_5H_4N$-2 (**6**), $C_5H_4N$-3 (**7**), and $C_5H_4N$-4 (**8**)], have been designed and synthesized to provide insight into the nature of the donor−acceptor interaction via a $\pi$-conjugated triple bond. The X-ray crystal structure of [TTF−(C≡C)−$C_6H_4OCH_3$-4] (**2**) reveals that the phenyl ring linked by acetylene is almost coplanar to the plane of TTF with a dihedral angle of 3.6°. The strong intermolecular C−H···O hydrogen bonding was found to direct the molecular helical assemblies with a screw pitch of 5.148 Å when viewed along the *a*-axis. Spectroscopic and electrochemical behaviors of the tetrathiafulvalene acetylene derivatives demonstrate that the TTF unit interacts with the electron-accepting group through the triple bond, thus leading to the intramolecular charge transfer. The pyridine-substituted TTF compounds **6**−**8** show remarkable sensing and coordinating properties toward $Pb^{2+}$. Comparison of the spectroscopic and electrochemical properties and the calculation at the B3LYP/6-31G* level available in Gaussian 03 reveals that varying the bridged unit of the TTF-$\pi$-A system from a double bond to a triple bond leads to positive shifts for the first and second oxidation potentials of the TTF moieties, while the extent of intramolecular charge transfer interactions through the $\pi$-conjugated triple bond is smaller than that through the double bond.

## Introduction

Over the past three decades, tetrathiafulvalene (TTF) and its derivatives have been extensively studied due to their unique $\pi$ electron-donating properties.[1−4] In addition to the famous intermolecular charge transfer complexes related to organic metals and electrically conducting materials,[2−3] TTF has been covalently linked to various electron-acceptor moieties.[2,4−12]

* Corresponding author. Tel.: 86-10-82543580. Fax: 86-10-82543580.

(1) (a) Wudl, F.; Smith, G. M.; Hufnagel, E. J. *J. Chem. Soc., Chem. Commun.* **1970**, 1453−1454. (b) Coleman, L. B.; Cohen, M. J.; Sandman, D. J.; Yamagishi, F. G.; Garito, A. F.; Heeger, A. J. *Solid State Commun.* **1973**, *12*, 1125−1132. (c) Narita, M.; Pittman, C. U., Jr. *Synthesis* **1976**, 489−513. (d) Otsubo, T.; Aso, Y.; Takimiya, K. *Adv. Mater.* **1996**, *8*, 203−211. (e) Wallis, J. D.; Griffiths, J. P. *J. Mater. Chem.* **2005**, *15*, 347−365.

10.1021/jo0622577 CCC: $37.00 
Published on Web 04/19/2007

Among them, TTF-$\pi$-A (A = acceptor) compounds have attracted much interest in recent years because the $\pi$-conjugated spacer is prone to optimize the communication between the TTF core and the acceptor group(s), and some of them have demonstrated promising potentials in a wide range of applications.[5−12] For example, Ouahab et al. systematically investigated the $\pi-$d interaction of the paramagnetic transition metal and organic donor of TTF-pyridine linked through a delocalized $\pi$ system, aimed at obtaining conducting and magnetic molecular-based materials.[5] Cassoux et al. adopted a $\pi$-conjugated double bond to bridge TTF and the *N*-methylpyridinium moiety, in which they observed an intramolecular charge transfer.[6] Martín et al. reported, in 1998, the first NLO materials containing the TTF unit as a donor moiety in D-$\pi$-A systems.[7] They found that the NLO properties have been improved upon introduction of the stronger electron acceptors into the TTF moiety. A low intensity of intramolecualr charge transfer appearing in the visible region was a prerequisite for the attainment of high $\beta$ values. Later, they described that $C_{60}$-based dyads bearing a $\pi$-extended TTF fragment displayed a long-lived photoinduced charge separation.[8] More recently, we took advantage of TTF as a donor in TTF-$\pi$-pyridine compound(s) to achieve highly selective colorimetric and electrochemical $Pb^{2+}$ detections.[9]

Very recently, TTF-$\pi$-A linked by triple $\pi$-conjugated bridge appeared at the forefront as a result of progress in synthetic TTF chemistry.[10−13] The Sonogashira reaction,[14] the palladium-catalyzed cross-coupling reaction of terminal alkynes with arylhalides, provides an efficient and versatile means of extending the $\pi-\pi$ conjugation. Despite the fact that the triple $\pi$-conjugated acetylene has been incorporated into a number of TTF derivatives,[10−11] little is known about the intramolecular electronic communication between TTF and acceptor associated with a triple bond as the linkage. Notably, Martín et al. recently demonstrated that through a simple exchange of C−C double bonds (oPPV) for C−C triple bonds (oPPE), the long-range photoinduced electron transfer (i.e., charge separation and charge recombination) in donor−acceptor conjugates could be considerably altered.[12] At the same time, Bryce et al. found that the absorption spectra of TTF−(C≡C)−OXD (OXD = 2,5-diphenyl-1,3,4-oxadiazole) hybrids are similar to the butadiynyl-OXD building block but blue-shifted by 80 nm as compared to the bithienyl-bridged derivative, implying that $\pi$ conjugation is disrupted by a neutral TTF unit.[13]

To gain insight into such an interaction, a series of TTF−(C≡C)−A (A = acceptor) compounds (**1**−**8**) (Scheme 1) have been designed and synthesized for understanding the fundamentals in this work. It is anticipated that (1) the rigid triple bond may simplify the electron communication between TTF and acceptor moiety in the ground state; (2) spectroscopic and electrochemical investigations may provide valuable information on such intramolecular interactions with subtle changes in the electron-accepting ability of the acceptors (i.e., benzene

(2) For reviews, see: (a) Jørgensen, T.; Hansen, T. K.; Becher, J. *Chem. Soc. Rev.* **1994**, *23*, 41−51. (b) Nielsen, M. B.; Lomholt, C.; Becher, J. *Chem. Soc. Rev.* **2000**, *29*, 153−164. (c) Segura, J. L.; Martín, N. *Angew. Chem., Int. Ed.* **2001**, *40*, 1372−1409. (d) Jeppesen, J. O.; Becher, J. *Eur. J. Org. Chem.* **2003**, 3245−3266. (e) Jeppesen, J. O.; Nielsen, M. B.; Becher, J. *Chem. Rev.* **2004**, *104*, 5115−5131. (f) El-Wareth, A.; Sarhan, A. O. *Tetrahedron* **2005**, *61*, 3889−3932.

(3) For reviews, see: (a) Williams, J. M.; Ferraro, J. R.; Thorn, R. J.; Carlson, K. D.; Geiser, U.; Wang, H. H.; Kini, A. M.; Whangbo, M. H. *Organic Superconductors (Including Fullerenes*); Prentice Hall: Engelwoods Cliffs, NJ, 1992. (b) Bryce, M. R. *Chem. Soc. Rev.* **1991**, *20*, 355−390. (c) Bryce, M. R. *J. Mater. Chem.* **1995**, *5*, 1481−1496. (d) Adam, M.; Müllen, K. *Adv. Mater.* **1994**, *6*, 439−459. (e) Khodorkovsky, V.; Becker, J. Y. In *Organic Conductors: Fundamentalsand Applications*; Farges, J. P., Ed.; Marcel Dekker: New York, 1994; Ch. 3, p 75. (f) Day, P.; Kurmoo, M. *J. Mater. Chem.* **1997**, *7*, 1291−1295.

(4) (a) Bryce, M. R. *Adv. Mater.* **1999**, *11*, 11−22. (b) Perepichka, D. F.; Bryce, M. R.; Pearson, C.; Petty, M. C.; McInnes, E. J. L.; Zhao, J. P. *Angew. Chem., Int. Ed.* **2003**, *42*, 4636−4639. (c) Nishikawa, H.; Kojima, S.; Kodama, T.; Ikemoto, I.; Suzuki, S.; Kikuchi, K.; Fujitsuka, M.; Luo, H.; Araki, Y.; Ito, O. *J. Phys. Chem. A* **2004**, *108*, 1881−1890. (d) Zhang, G. X; Zhang, D. Q.; Guo, X. F.; Zhu, D. B. *Org. Lett.* **2004**, *6* (8), 1209−1212. (e) Xiao, X. W.; Xu, W.; Zhang, D. Q.; Xu, H.; Liu, L.; Zhu, D. B. *New J. Chem.* **2005**, *29* (10), 1291−1294. (f) Tsiperman, E.; Becker, J. Y.; Khodorkovsky, V.; Shames, A.; Shapiro, L. *Angew. Chem., Int. Ed.* **2005**, *44*, 4015−4018. (g) Jia, C. Y.; Liu, S. X.; Tanner, C.; Leiggener, C.; Sanguinet, L.; Levillain, E.; Leutwyler, S.; Hauser, A.; Decurtins, S. *Chem. Commun.* **2006**, 1878−1880.

(5) (a) Iwahori, F.; Golhen, S.; Ouahab, L.; Carlier, R.; Sutter, J. -P. *Inorg. Chem.* **2001**, *40*, 6541−6542. (b) Ouahab, L.; Iwahori, F.; Golhen, S.; Carlier, R.; Sutter, J.-P. *Synth. Met.* **2003**, *133*−*134*, 505−507. (c) Setifi, F.; Ouahab, L.; Golhen, S.; Yoshida, Y.; Saito, G. *Inorg. Chem.* **2003**, *42*, 1791−1793.

(6) Andreu, R.; Malfant, I.; Lacroix, G. P.; Cassoux, P. *Eur. J. Org. Chem.* **2000**, 737−741.

(7) (a) de Lucas, A. I.; Martín, N.; Sánchez, L.; Seoane, C.; Andreu, R.; Garín, J.; Orduna, J.; Alcalá, R.; Villacampa, B. *Tetrahedron* **1998**, *54*, 4655−4662. (b) Garín, J.; Orduna, J.; Rupérez, J. I.; Alcalá, R.; Villacampa, B.; Sánchez, C.; Martín, N.; Segura, J. L.; González, M. *Tetrahedron Lett.* **1998**, *39*, 3577−3580. (c) González, M.; Martín, N.; Segura, J. L.; Seoane, C.; Garín, J.; Orduna, J.; Alcalá, R.; Sánchez, C.; Villacampa, B. *Tetrahedron Lett.* **1999**, *40*, 8599−8602. (d) Bryce, M. R.; Green, A.; Moore, A. J.; Perepichka, D. F.; Batsanov, A. S.; Howard, J. A. K.; Ledoux-Rak, I.; González, M.; Martín, N.; Segura, J. L.; Garín, J.; Orduna, J.; Alcalá, R.; Villacampa, B. *Eur. J. Org. Chem.* **2001**, 1927−1935. (e) González, M.; Segura, J. L.; Seoane, C.; Martín, N. *J. Org. Chem.* **2001**, *66*, 8872−8882. (f) Otero, M.; Herranz, M. Á.; Seoane, C.; Martín, N.; Garín, J.; Orduna, J.; Alcalá, R.; Villacampa, B. *Tetrahedron* **2002**, *58*, 7463−7475. (g) Insuasty, B.; Atienza, C.; Seoane, C.; Martín, N.; Garín, J.; Orduna, J.; Alcalá, R.; Villacampa, B. *J. Org. Chem.* **2004**, *69*, 6986−6995.

(8) (a) Martín, N.; Pérez, I.; Sánchez, L.; Seoane, C. *J. Org. Chem.* **1997**, *62*, 5690−5695. (b) Herranz, M. Á.; Illescas, B.; Martín, N. *J. Org. Chem.* **2000**, *65*, 5728−5738. (c) Martín, N.; Sánchez, L.; Herranz, M. A. *J. Phys. Chem. A* **2000**, *104*, 4648−4657. (d) González, S.; Martín, N. *J. Org. Chem.* **2003**, *68*, 779−791. (e) Sánchez, L.; Pérez, I.; Martín, N.; Guldi, D. M. *Chem.*−*Eur. J.* **2003**, *9*, 2457−2468. (f) Giacalone, F.; Segura, J. L.; Martín, N.; Guldi, D. M. *J. Am. Chem. Soc.* **2004**, *126*, 5340−5341. (g) Giacalone, F.; Segura, J. L.; Martín, N.; Ramey, J.; Guldi, D. M. *Chem.*−*Eur. J.* **2005**, *11*, 4819−4834. (h) Herranz, M. Á.; Martín, N.; Campidelli, S.; Prato, M.; Brehm, G.; Guldi, D. M. *Angew. Chem., Int. Ed.* **2006**, *45*, 4478−4482.

(9) Xue, H.; Tang, X. J.; Wu, L. Z.; Zhang, L. P.; Tung, C. H. *J. Org. Chem.* **2005**, *70*, 9727−9734 and references therein.

(10) (a) Iyoda, M.; Hasegawa, M.; Miyake, Y. *Chem. Rev.* **2004**, *104*, 5085−5113. (b) Wang, C. S.; Batsanov, A. S.; Bryce, M. R. *Chem. Commun.* **2004**, 578−579. (c) Hasegawwa, M.; Takano, J.; Enozawa, H.; Kuwatani, Y.; Iyoda, M. *Tetrahedron Lett.* **2004**, *45*, 4109−4112. (d) Hara, K.; Hasegawa, M.; Kuwatani, Y.; Enozawa, H.; Iyoda, M. *Chem. Commun.* **2004**, 2042−2043. (e) Enozawa, H.; Hasegawa, M.; Takamatsu, D.; Fukui, K.; Iyoda, M. *Org. Lett.* **2006**, *8*, 1917−1920. (f) Nielsen, M. B.; Moonen, N. N. P.; Boudon, C.; Gisselbrecht, J. P.; Seiler, P.; Gross, M.; Diederich, F. *Chem. Commun.* **2001**, 1848−1849. (g) Nielsen, M. B.; Utesch, N. F.; Moonen, N. N. P.; Boudon, C.; Gisselbrecht, J.-P.; Concilio, S.; Piotto, S. P.; Seiler, P.; Günter, P.; Gross, M.; Diederich, F. *Chem.*−*Eur. J.* **2002**, *8*, 3601−3613. (h) Andersson, A. S.; Kilsa, K.; Hassenkam, T.; Gisselbrecht, J.; Boudon, C.; Gross, M.; Nielsen, M. B.; Diederich, F. *Chem.*−*Eur. J.* **2006**, *12*, 8451−8459.

(11) (a) Otsubo, T.; Kochi, Y.; Bitoh, A.; Ogura, F. *Chem. Lett.* **1994**, 2047−2050. (b) Yamamoto, T.; Shimizu, T. *J. Mater. Chem.* **1997**, *7*, 1967−1968. (c) Solooki, D.; Parker, T. C.; Khan, S. I.; Rubin, Y. *Tetrahedron Lett.* **1998**, *39*, 1327−1330. (d) Iyoda, M.; Hasegawa, M.; Takano, J.; Hara, K.; Kuwatani, Y. *Chem. Lett.* **2002**, 590−591. (e) Iyoda, M.; Enozawa, H.; Miyake, Y. *Chem. Lett.* **2004**, 1098−1099. (f) Chen, G.; Zhao, Y. M. *Tetrahedron Lett.* **2006**, *47*, 5069−5073.

(12) Atienza, C.; Martín, N.; Wielopolski, M.; Haworth, N.; Clark, T.; Guldi, D. M. *Chem. Commun.* **2006**, 3202−3204.

(13) Wang, C. S.; Pålsson, L.-O.; Batsanov, A. S.; Bryce, M. R. *J. Am. Chem. Soc.* **2006**, *128*, 3789−3799.

(14) (a) Sonogashira, K. In *Comprehensive Organic Synthesis*; Trost, B. M., Fleming, I., Eds.; Pergamon Press: Oxford, 1991; Vol. 3, p 521. (b) Sonogashira, K. In *Metal-Catalyzed Cross-Coupling Reactions*; Diederich, F., Stang, P. J., Eds.; Wiley-VCH: Weinheim, 1998; p 203. (c) Sonogashira, K. *J. Organomet. Chem.* **2002**, *653*, 46−49.

**SCHEME 1. Synthetic Route of 1−8**

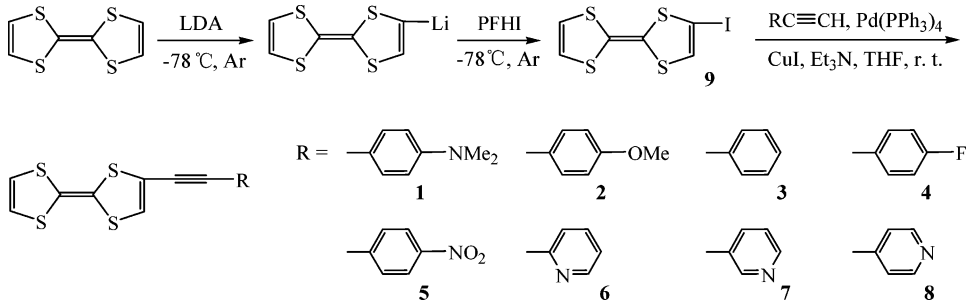


derivatives and pyridine) in TTF−(C≡C)−A compounds because the intramolecular charge transfer interaction is the most frequently manifested in the optical and electrochemical properties; and (3) it has been known that the intramolecular charge transfer shows remarkable sensing and coordinating properties to $Pb^{2+}$ with respect to our recent observations on TTF-$\pi$-pyridine derivatives bridged by a double bond.[9] Therefore, $Pb^{2+}$ ions are expected not only to complex with a monodentate pyridine moiety displaying high selectivity but also to serve as an external stimulus probing the extent of $\pi$ conjugation of TTF-$\pi$-A systems with the triple bond and double bond as the linkage, respectively.

In the present work, we report that a $\pi$-conjugated triple bond can act as a bridge to optimize the communication between TTF moiety and acceptors, thus leading to the intramolecular charge transfer state. The absorption energy and substantial oxidation potentials of TTF are sensitive to the subtle changes of the electron-accepting ability of the acceptors and the polarity of the solvents used. The interaction of pyridyl-substituted TTF compound(s) with an external stimulus of $Pb^{2+}$ ions can modulate the intramolecular charge transfer, resulting in remarkable changes in the absorption spectra, $^1$H NMR spectra, and electrochemical properties. Varying the bridged unit of the TTF-$\pi$-A system from a double bond to a triple bond leads to positive shifts for the first and second oxidation potentials of the TTF moieties, while the extent of $\pi$ conjugation of the TTF−(C≡C)−A systems is relatively smaller as compared to the double bond-bridged compounds.

## Results and Discussion

**Synthesis.** The syntheses of **1**−**8** were carried out under typical Sonogashira coupling conditions[14] (Scheme 1). As reported in the literature, the starting material 2-iodotetrathiafulvalene (**9**)[15] was prepared by treatment of the tetrathiafulvalenyllithium[16] with perfluorohexyl iodide (PFHI) at −60 °C under argon conditions. Reaction of **9** with HC≡CR in the mixed solvent of $NEt_3$ and anhydrous THF for 5 h, catalyzed by CuI and $Pd(PPh_3)_4$ at room temperature, afforded compounds of **1**−**8** as a yellow to red crystal with a good to excellent yield of 50−92%, respectively. Compared with the $\pi$-bridged analogue bearing double bond,[9] the synthesis can be performed under mild conditions with a relatively shorter reaction time but higher yields. $^1$H NMR and $^{13}$C NMR spectroscopies, MS spectrometry, and satisfactory elemental analyses confirmed the identities of all the compounds. The crystal structure of **2** was also determined.

**X-ray Crystal Structure Determination of 2.** Single crystals of **2** have been obtained by diffusion of hexane into the $CH_2Cl_2$ solution of **2** and determined by X-ray diffraction. A yellow single crystal as a plate with dimensions of 0.24 mm × 0.20 mm × 0.16 mm was used for data collection at 294 K. The molecular structure and packing diagram of **2** are depicted in Figure 1. The crystal belongs to the orthorhombic crystal system $P2(1)2(1)2(1)$ with unit cell parameters of $a = 5.148(2)$ Å, $b = 10.506(5)$ Å, $c = 27.520(12)$ Å, $\alpha = 90°$, $\beta = 90°$, and $\gamma = 90°$. As shown in Figure 1, **2** lies almost on the same plane. The C≡C bond length of 1.209(4) Å is comparable to that of other similar C≡C bonds (1.203(5) Å) in the literature.[10b] The phenyl ring of acetylene is almost coplanar to the plane of the TTF moiety with a dihedral angle of 3.6° (C9−C10−C5−C6). The TTF moiety has a slightly twisted cis-conformation with dihedral angles of 0.6° (C5−C6−C4−C3) and 10.2° (C4−C3−C1−C2), respectively. A noticeable feature of the TTF moiety lies in two bond lengths of 1.725(3) Å (S(3)−C(5)) and 1.343(4) Å (C(5)−C(6)). All the other S−C bonds in **2** (between 1.743(3) and 1.780(3) Å) are significantly longer than S(3)−C(5), and the non-conjugated C(1)−(2) bond (1.303(5) Å) is shorter than C(5)−C(6), indicating that the whole triple bond-bridged TTF-$\pi$-A compound of **2** is significantly conjugated. Interestingly, the strong intermolecular C−H···O hydrogen bonding was found to direct the molecular packing. Each molecule of **2** is stacked with two adjacent molecules in a head-to-head manner (Figure 1b). The H···O distance (2.57 Å) in the observed C−H···O hydrogen bonding is appreciably shorter than the sum of the van der Waals radii for H (1.20 Å) and O (1.52 Å), respectively. The intermolecular contact of 3.518 Å at C15B−H15B···O1A with a C−H···O angle of 168.63(21)° leads to the formation of helical assemblies with screw pitch of 5.148 Å when viewed along the *a*-axis. The path of the helix can be easily traced by following the hydrogen bonds counterclockwise around the screw axis of the helix (Figure 1c).

**Spectroscopic and Electrochemical Properties of 1−5.** The absorption spectra of **1**−**5** as well as the parent compound TTF in acetonitrile solution were investigated and are shown in Figure 2. All these compounds display intense absorptions at $\lambda < 370$ nm with extinction coefficients on the order of $10^4$ dm$^3$ mol$^{-1}$ cm$^{-1}$. Moderately intense low-energy absorptions in the region of 370−600 nm were observed for **1**−**5**, while the same feature was absent for the parent compound of TTF. The absorption spectral properties follow Beer's Law at concentrations below $1 \times 10^{-4}$ mol/L, suggesting that no aggregation occurred. Significantly, the absorption spectra of **1**−**5** are different from that of the two-component (TTF and arylacetylene) mixture under the same conditions, implying that the triple bond linkage modulated the electron distribution in **1**−**5**. With reference to previous works on the double bond-bridged

(15) Wang, C. S.; Ellern, A.; Khodorkovsky, V.; Bernstein, J.; Becker, J. Y. *J. Chem. Soc., Chem. Commun.* **1994**, 983−984.
(16) Green, D. C. *J. Org. Chem.* **1979**, *44*, 1476−1479.

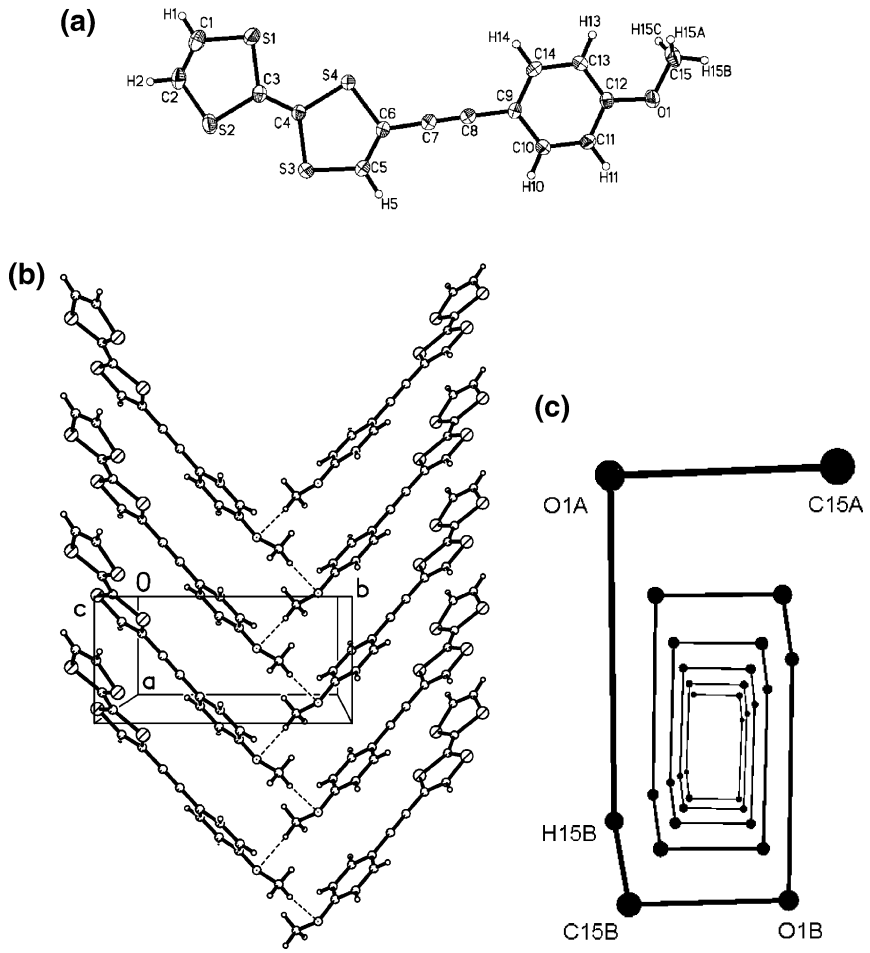


**FIGURE 1.** (a) Perspective drawing of **2** with atomic numbering. (b) Packing diagram of **2**. (c) Helix diagram viewed along the *a*-axis; only C, H, and O atoms are retained for clarity.

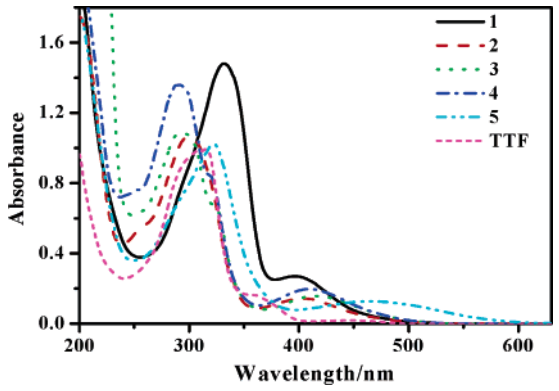


**FIGURE 2.** Absorption spectra of compounds **1**−**5** and the parent TTF in $CH_3CN$ solution ($10^{-5}$ mol/L) at room temperature.

TTF-$\pi$-A compounds,[9] the absorptions at $\lambda$ < 370 nm are assigned to the local transition in the TTF moiety, while the low-energy absorption at 370−600 nm may arise from the intramolecular charge transfer. Compound **1**, which has an electron-rich *N*,*N*-dimethyl substituent, shows the maximum of the low-energy absorption at 396 nm, while **5**, with the most electron-poor nitro group, shows the maximum of the low-energy absorption at 465 nm (Figure 2). Table 1 lists the maximum absorption wavelength ($\lambda_{max}$) of **1**−**5** in different polarities of solvents. It was noted that the lowest absorption energies of **1**−**5** in solution depend on the nature of the substituents on the phenyl ring. The stronger the electron-accepting ability of the substituent is, the lower the energy of absorption will be. Moreover, **1**−**5** are substantially blue-shifted, spanning over 10−20 nm along the polarity of solvents, indicating the occurrence of intramolecular charge transfer. Therefore, the triple bond as a bridge is promising to extend conjugation of a whole molecule, to optimize the electronic communication between TTF moiety and acceptors, and to produce an intramolecular charge transfer state.

**TABLE 1. Maximum Absorption Wavelength[a] of 1−5 in Various Solvents**

| | 1 | 2 | 3 | 4 | 5 |
|---|---|---|---|---|---|
| $C_6H_6$ | 405 | 414 | 421 | 416 | 480 |
| $CH_2Cl_2$ | 402 | 410 | 416 | 414 | 476 |
| $CH_3OH$ | 396 | 405 | 413 | 410 | 468 |
| $CH_3CN$ | 396 | 403 | 411 | 409 | 465 |

[a] $\lambda_{max}$ (nm).

It has been well-known that TTF derivatives can undergo two successive reversible 1e oxidations to the $TTF^{+\cdot}$ radical and $TTF^{2+}$ species at $E^1_{ox}$ and $E^2_{ox}$ ($E^1_{1/2}$ = 0.37 V and $E^2_{1/2}$ = 0.67 V vs SCE, in $CH_2Cl_2$ solution), respectively. All the compounds show two reversible one-electron oxidation waves, and the potentials are shifted to higher positive values relative to the parent TTF. Table 2 summarizes the oxidative potentials of **1**−**5**, together with the parent compound TTF. Evidently, the stronger electron-accepting group of the nitro group

**TABLE 2. Oxidative Potentials (mV vs SCE) of 1−5 and Parent TTF in $CH_3CN$ with $^nBu_4NPF_6$ (0.1 mol/L) as Supporting Electrolyte (100 mV/s)**

| | TTF | 1 | 2 | 3 | 4 | 5 |
|---|---|---|---|---|---|---|
| $E^1_{ox}$ | 384 | 414 | 432 | 449 | 460 | 473 |
| $E^2_{ox}$ | 768 | 762 | 790 | 807 | 825 | 842 |

presented in **5** affords the oxidation of **5** ($E^1_{ox}$ = 473 mV vs SCE and $E^2_{ox}$ = 842 mV vs SCE, in $CH_3CN$ solution) occurring at more positive potentials than that of **1** ($E^1_{ox}$ = 414 mV vs SCE and $E^2_{ox}$ = 762 mV vs SCE, in $CH_3CN$ solution). The intramolecular charge transfer from the TTF unit to the acceptor moiety decreases the electron density of TTF and makes the oxidation of TTF less favorable. The sensitivity of the potentials toward the nature of the different substituents on the phenyl ring is due to the intramolecular charge transfer delocalization occurring in these compounds.

**$Pb^{2+}$-Binding Properties of 6−8.** As demonstrated previously, upon introduction of a $\pi$-conjugated triple bond as the linkage to TTF-$\pi$-A molecules, TTF and the acceptor moiety can interact with each other through-bond, forming the intramolecular charge transfer state. To shed more light on the intramolecular charge transfer characteristics in nature, **6**−**8** bearing a monodentate pyridyl ligand have also been taken into consideration. 2-,3-,4-Pyridyl-substituted groups here serve as both electron-accepting groups and receptors for recognition event. Similar to **1**−**5**, **6**−**8** also exhibit the typical absorption and electrochemical characteristics of the intramolecular charge transfer (Table S2). Moreover, the intramolecualr charge transfer energy was found to rely on the substituted position of the pyridyl group. 4-Pyridyl-substituted **8** with the strongest electron-accepting ability gives the lowest absorption energy in **6**−**8**.

The salient results obtained from pyridyl-substituted **6**−**8** are remarkable sensing and coordinating properties in the case of $Pb^{2+}$. An initial observation when working with an acetonitrile solution of **8** was the change of the yellow color to deep purple when exposed to a micromolar concentration of $Pb(ClO_4)_2$. UV−vis spectroscopy, $^1$H NMR, and cyclic voltammetry were used to evaluate the binding properties of the pyridyl **6**−**8** toward cations. Figure 3 presents the absorption spectra of **6**−**8** in acetonitrile (0.1 mol/L $^nBu_4NPF_6$) as a function of added $Pb(ClO_4)_2$. Upon addition of $Pb^{2+}$ to the solution of **8**, the decrease in the absorption at 432 nm was accompanied by a growth with a maximum at 550 nm (Figure 3a). Well-defined isosbestic points at 312, 382, and 472 nm were observed, indicative of the presence of only two absorbing species in the solution, the free **8** and the complex **8**·$Pb^{2+}$. At the end of the titration, the solution changed from yellow to purple. The intramolecular charge transfer responsive to the external cation stimulus exhibits a bathochromic shift for about 118 nm. Spectroscopic recognition of $Pb^{2+}$ to the pyridyl unit was confirmed by the absence of spectral changes in the absorption spectrum of phenyl-substituted **3**. Therefore, the interaction between the pyridyl group and the $Pb^{2+}$ ion increases the electron-accepting ability of the pyridyl group and shifts the intramolecular charge transfer to a lower energy. The red-shift in the absorption spectrum suggests that the whole molecule of TTF−(C≡C)−pyridine is conjugated. The inset in Figure 3a gives the plot of $A$ versus [$Pb^{2+}$], where $A$ and $A_0$ refers to the absorbance at 550 nm for **8** in the presence and absence of $Pb^{2+}$. The 1:1 stoichiometry for $Pb^{2+}$ ion binding by **8** was evidenced by the close agreement of the experimental data with the theoretical fit according to

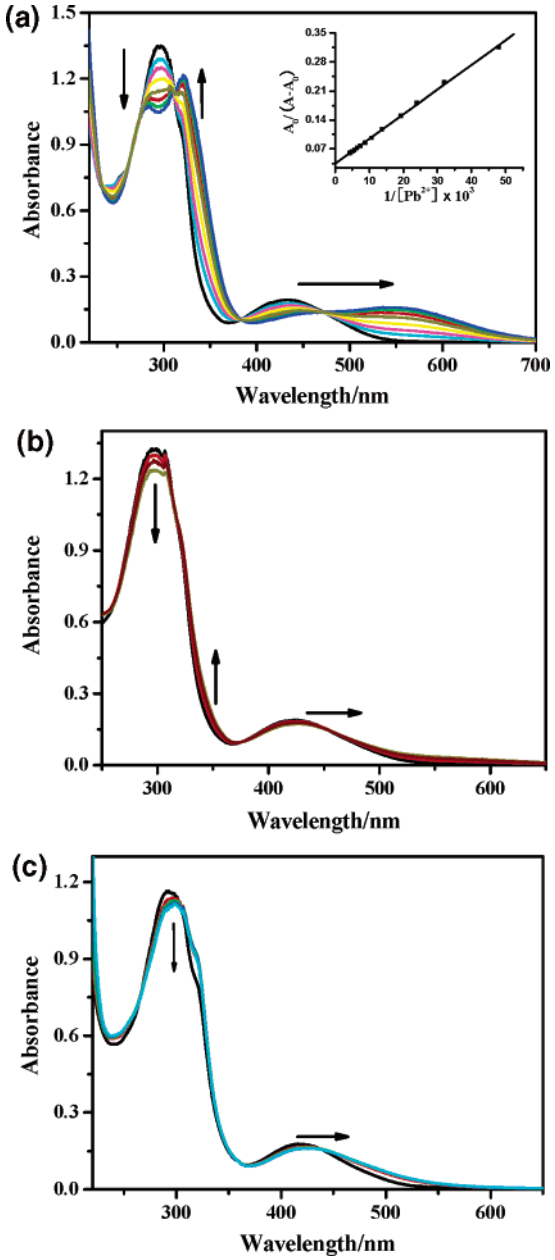


**FIGURE 3.** Absorption spectra of **6**−**8** in $CH_3CN$ with 0.1 mol/L $^nBu_4NPF_6$ as a function of the concentration of $Pb^{2+}$ (0−2.3 × $10^{-4}$ mol/L). (a) **8** (5.0 × $10^{-5}$ mol/L); (b) **6** (5.4 × $10^{-5}$ mol/L); and (c) **7** (5.0 × $10^{-5}$ mol/L). The inset shows the titration curve by the plot of the absorbance at 550 nm for **8** against [$Pb^{2+}$].

the Hildebrand−Benesi equation (eq 1).[17] The binding constant log $K_s$ determined from such plots for $Pb^{2+}$ is 3.76 in acetonitrile. Other metal ions, such as $Zn^{2+}$, $Cd^{2+}$, alkali, and alkaline earth metal cations, do not affect the absorption spectrum of **8**. Similar changes in the absorption spectra were also observed for **6** and **7** upon addition of $Pb^{2+}$. However, these changes in **6** and **7** are smaller than that of **8**. Obviously, the complexation between the 2- and 3-pyridyl in **6** and **7** with $Pb^{2+}$ also leads to the increase in the electron-accepting ability of the pyridine, but the extents are much smaller than that of **8**. The 1:1 stoichiometry for $Pb^{2+}$ by **6** and **7** (Figure S2) was in

(17) Connors, K. A. *Binding Constant: The Measurement of Molecular Complex Stability*; John Wiley and Sons: New York, 1987.

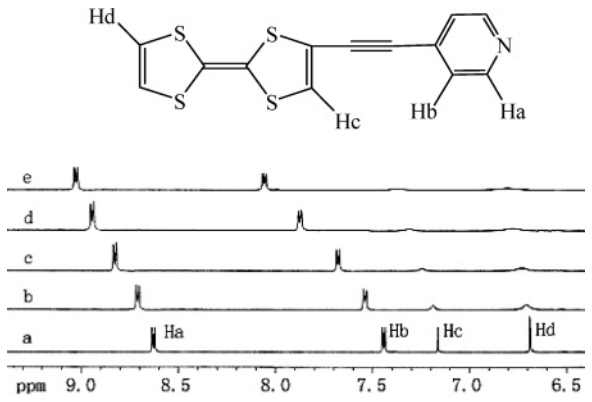


**FIGURE 4.** $^1$H NMR spectra of **8** ($4.3 \times 10^{-3}$ mol/L) in $CD_3COCD_3$ as a function of $Pb^{2+}$ concentration. [$Pb^{2+}$]: (a) 0; (b) 0.4 equiv; (c) 1.0 equiv; (d) 2.6 equiv; and (e) 4.0 equiv.

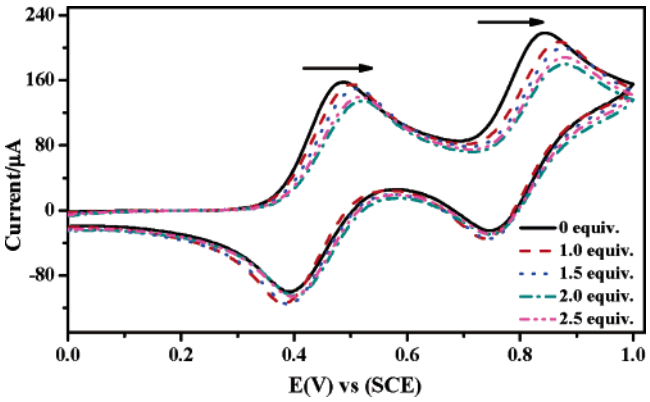


**FIGURE 5.** Cyclic voltammogram of **8** ($10^{-3}$ mol/L) as a function of $Pb^{2+}$ concentration, recorded in a mixture of $CH_3CN$ with $^nBu_4NPF_6$ (0.1 mol/L) as the supporting electrolyte.

close agreement with the experimental data according to the Hildebrand−Benesi equation (eq 1).[17] The contrast between their binding constants (log $K_s$) also proves that the more favorable conjugation and less steric hindrance of the 4-pyridyl-substituted group in **8** result in a higher binding constant of **8** (3.76) than those of **6** (1.7) and **7** (2.76), respectively.

The chemical shifts of the resonances associated with the pyridyl protons in $^1$H NMR spectra of **8** show significant changes upon complexation with $Pb^{2+}$ (Figure 4). The signals of the protons in the TTF moiety shift downfield and become broad, but the shifts are smaller as compared with those for pyridyl protons. At the same time, the addition of $Pb^{2+}$ to the solution of **3** under identical conditions did not cause any changes in the chemical shift of the $^1$H NMR spectra except for the signals of TTF moiety broadening. These observations confirm that $Pb^{2+}$ interacts with the pyridyl group and that the whole molecule of **8** is a conjugated system. The $^1$H NMR spectral changes in **6** and **7** also shift downfield upon addition of $Pb^{2+}$, but the extents are less than in the case of **8** (Figures S3 and S4).

The progressive addition of $Pb(ClO_4)_2$ to the solution of **8** in $CH_3CN$ with $^nBu_4NPF_6$ (0.1 mol/L) causes significant modifications in CVs, and substantial positive shifts from 484 to 520 mV for the first oxidation potential, and from 839 to 879 mV for the second oxidation potential, respectively, were observed (Figure 5). Evidently, the complexation of $Pb^{2+}$ increases the electron-accepting ability of the pyridyl group

**TABLE 3. Oxidative Potential Data of 6−8 in $CH_3CN$ in Presence and Absence of $Pb^{2+}$, Recorded at 298 K with $^nBu_4NPF_6$ (0.1 mol/L) as Supporting Electrolyte**

| | **6** | **6** + $Pb^{2+}$ [a] | **7** | **7** + $Pb^{2+}$ [a] | **8** | **8** + $Pb^{2+}$ [b] |
|---|---|---|---|---|---|---|
| $E^1_{ox}$ (mV) | 478 | 486 | 464 | 481 | 484 | 520 |
| $E^2_{ox}$ (mV) | 833 | 848 | 825 | 843 | 839 | 879 |

[a] In the presence of 5 equiv of $Pb^{2+}$. [b] In the presence of 2.5 equiv of $Pb^{2+}$.

**TABLE 4. Comparison of Spectroscopic and Electrochemical Properties and Calculation of TTF-$\pi$-A Derivatives Bearing Double and Triple Bonds, Respectively**

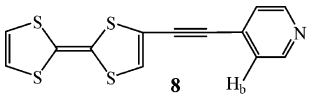


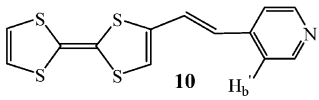


| | | **8** | **10** |
|---|---|---|---|
| $\lambda_{max}$ (nm)[a] | | 432 (429)[b] | 440 (435)[b] |
| | +$Pb^{2+}$ | 550 | 555 |
| $^1$H NMR (ppm)[c] | | $H_b$ = 7.45 | $H_b'$ = 7.62 |
| | +$Pb^{2+}$ | $H_b$ = 8.07 | $H_b'$ = 8.40 |
| | $\Delta\delta$ | $\Delta\delta$ ($H_b$) = 0.62 | $\Delta\delta$ ($H_b'$) = 0.78 |
| $E^1_{ox}$ (mV)[d] | | 484 | 440 |
| | +$Pb^{2+}$ | 520 | 510 |
| | $\Delta E^1_{ox}$ | 36 | 70 |
| $E^2_{ox}$ (mV)[d] | | 839 | 805 |
| | +$Pb^{2+}$ | 879 | 885 |
| | $\Delta E^2_{ox}$ | 40 | 80 |

[a] Experimental determined value in $CH_3CN$ solution ($10^{-5}$ mol/L) at room temperature. [b] Calculation determined value from the respective HOMO and LUMO at B3LYP/6-31G* level available as Gaussian 03 package. [c] In $CD_3COCD_3$ solution. [d] In a mixture of $CH_3CN$ with $^nBu_4NPF_6$ (0.1 mol/L) as the supporting electrolyte (vs SCE).

in **8**, resulting in the decrease of electron density in the TTF unit. The alteration of the second oxidation potential suggests that the charged $TTF^{2+}$ cation should not be in close proximity to the metallic ion of $Pb^{2+}$. This observation is in contrast to the TTF-macrocyclic systems,[2] where the second oxidation potential remained unchanged owing to the increased repulsive electrostatic interaction. Similar changes in the CV spectra were also observed for compounds **6** and **7** upon addition of $Pb^{2+}$. However, these changes in **6** and **7** are much smaller than that of **8** (Table 3). No perturbation of the CVs of **6**−**8** was observed upon addition of group 1 or 2 cations.

**Comparison of TTF-$\pi$-A Compounds Bearing $\pi$-Conjugated Double Bond or Triple Bond Bridge.** It is pertinent to compare the spectroscopic, electrochemical, and $Pb^{2+}$-binding properties of TTF−(C≡C)−A described in this work with those analogues bearing a double bond bridge. For the latter, which exhibits strong absorption in the range of 370−550 nm with $\lambda_{max}$ at 440 nm, and the two typical positive shifted oxidation potentials of the TTF unit (Table 4), the intramolecular charge transfer has been well-established.[6−9] Similar behaviors observed in the TTF−(C≡C)−A analogues suggest that the TTF unit interacts with the electron-accepting moiety through a triple bond.

To provide a comparative study on the donor−acceptor interaction, detailed spectroscopic and electrochemical studies have been carried out on the 4-pyridyl-substituted compounds of **8** and **10**. As shown in Table 4, varying the bridged unit from double bond **10** to triple bond **8** leads to 44 and 34 mV positive shifts for the first and second oxidation potentials, respectively. The chemical shift of the resonance associated with the pyridyl proton of $H_b$ in **8** is upfield shifted 0.17 ppm as compared with that of **10**. These facts may be ascribed to the

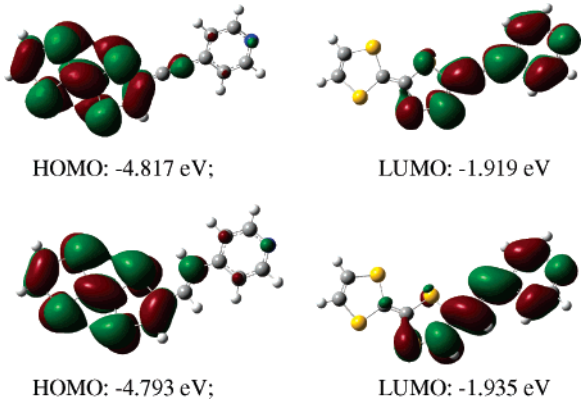


**FIGURE 6.** Molecular orbital scheme of the HOMO and LUMO of **8** (top) and **10** (bottom).

stronger electron affinity of the triple bond resulting in a larger decrease in electron density of the TTF unit and subsequently enhancing the oxidation of TTF at higher potentials.

The calculations at the density functional theory B3LYP/6-31G* level,[18] available in Gaussian 03,[19] were carried out to understand that intramolecular charge transfer existed in **8** and **10**. The molecules **8** (top) and **10** (bottom) lie almost on the same plane, respectively, in favor of the conjugation between TTF moiety and pyridyl unit. The frontier orbital resulting from the calculations is presented in Figure 6. It is clear that the HOMO in both molecules of **8** and **10** is mainly localized on the TTF moiety and that the LUMO lies on the pyridyl group and $\pi$-conjugated bridge unit. Although structurally similar, the energy of the HOMO in **8** (−4.817 eV) is slightly lower than that in **10** (−4.793 eV), while the energy of the LUMO in **8** (−1.919 eV) is higher than that in **10** (−1.935 eV). As a result, there are obvious differences in the intramolecular charge transfer energies in **8** and **10**. Good agreement between calculation and experiments (Table 4) further illustrates the contributions of TTF and the accepting group involved in the charge transfer characters.

Alternatively, $Pb^{2+}$ ions are employed as an external stimulus to probe the extent of donor−acceptor interactions associated with the double or triple bond bridge. Obviously, with the addition of a micromolar concentration of $Pb^{2+}$ ions to the solution, **8** and **10** display dramatic changes in the UV−vis absorption spectrum, $^1$H NMR spectrum, and redox property. However, addition of $Pb^{2+}$ in **8** results in (1) only a smaller increase in the oxidation potentials (36 mV for the first and 40 mV for the second waves) as compared with those of **10** (70 mV for the first and 80 mV for the second waves) and (2) smaller downfield shift for **8** [$\Delta\delta$ ($H_b$) 0.62 ppm] than that of **10** [$\Delta\delta$ ($H_b'$) 0.78 ppm] in the $^1$H NMR spectra, in spite of similar red-shifts observed in their absorption spectra. Therefore, it can be speculated that the extent of donor−acceptor interactions through the triple bond is smaller than the similar analogue bearing double bond.

(18) (a) Becke, A. D. *Phys. Rev. A* **1988**, *38*, 3098−3100. (b) Lee, C.; Yang, W.; Parr, R. G. *Phys. Rev. B* **1988**, *37*, 785−789.

(19) Frisch, M. J.; Trucks, G. W.; Schlegel, H. B.; Scuseria, G. E.; Robb, M. A.; Cheeseman, J. R.; Montgomery, J. A., Jr.; Vreven, T.; Kudin, K. N.; Burant, J. C.; Millam, J. M.; Iyengar, S. S.; Tomasi, J.; Barone, V.; Mennucci, B.; Cossi, M.; Scalmani, G.; Rega, N.; Petersson, G. A.; Nakatsuji, H.; Hada, M.; Ehara, M.; Toyota, K.; Fukuda, R.; Hasegawa, J.; Ishida, M.; Nakajima, T.; Honda, Y.; Kitao, O.; Nakai, H.; Klene, M.; Li, X.; Knox, J. E.; Hratchian, H. P.; Cross, J. B.; Adamo, C.; Jaramillo, J.; Gomperts, R.; Stratmann, R. E.; Yazyev, O.; Austin, A. J.; Cammi, R.; Pomelli, C.; Ochterski, J. W.; Ayala, P. Y.; Morokuma, K.; Voth, G. A.; Salvador, P.; Dannenberg, J. J.; Zakrzewski, V. G.; Dapprich, S.; Daniels, A. D.; Strain, M. C.; Farkas, O.; Malick, D. K.; Rabuck, A. D.; Raghavachari, K.; Foresman, J. B.; Ortiz, J. V.; Cui, Q.; Baboul, A. G.; Clifford, S.; Cioslowski, J.; Stefanov, B. B.; Liu, G.; Liashenko, A.; Piskorz, P.; Komaromi, I.; Martin, R. L.; Fox, D. J.; Keith, T.; Al-Laham, M. A.; Peng, C. Y.; Nanayakkara, A.; Challacombe, M.; Gill, P. M. W.; Johnson, B.; Chen, W.; Wong, M. W.; Gonzalez, C.; Pople, J. A. *Gaussian 03*, Revision B.05; Gaussian, Inc.: Pittsburgh PA, 2003.

## Conclusion

The Sonogashira reaction was employed to synthesize a series of TTF-$\pi$-A derivatives bridged via a $\pi$-conjugated triple bond. The synthesis can be performed under mild conditions with a relatively short reaction time, but the yields are higher as compared to the $\pi$-bridged analogue bearing double bond. The X-ray crystal structure of **2** reveals that the phenyl ring linked by acetylene is almost coplanar to the plane of TTF with a dihedral angle of 3.6°. The strong intermolecular C−H···O hydrogen bonding was found to direct the molecular helical assemblies with a screw pitch of 5.148 Å when viewed along the *a*-axis. Spectroscopic, electrochemical, and $Pb^{2+}$-binding studies demonstrate that the triple bond is effective in optimizing the electronic communication between TTF moiety and acceptors, thus leading to intramolecular charge transfer, of which the absorption energy and substantial oxidation potentials are sensitive to the changes of the electron-accepting ability of the acceptor moiety and polarity of solvents. The interaction of pyridyl-substituted TTF compound(s) with metal ions can significantly modulate the intramolecular charge transfer state, resulting in remarkable changes in the solution color from yellow to bluish purple, $^1$H NMR spectra, and electrochemical properties. Comparison of the spectroscopic and electrochemical properties and the calculation at the B3LYP/6-31G* level reveals that the nature of the spacer linking TTF and acceptor moiety has a profound impact on the intramolecular charge transfer state. Varying the bridged unit of the TTF-$\pi$-A system from a double bond to a triple bond leads to positive shifts for the first and second oxidation potentials of the TTF moieties, while the extent of the donor−acceptor interaction through the triple bond is smaller than the similar analogue bearing double bond.

## Experimental Section

**Materials and Reagents.** Tetrathiafulvalenyllithium and 2-iodotetrathiafulvalene (**9**) were prepared according to literature methods.[15,16] Tetrahydrofuran (THF) and diethyl ether ($Et_2O$) were used after refluxing for 10 h in the presence of sodium. Other reagents were of analytical grade and were used as received.

**4-(Tetrathiafulvalenylethynyl)-*N*,*N*-dimethylbenzenamine (1).** Compound **9** (100 mg, 0.3 mmol), 4-ethynyl-*N*,*N*-dimethylbenzenamine (44 mg, 0.3 mmol), $Pd(PPh_3)_4$ (17 mg), and CuI (6.0 mg) were added to a solution of anhydrous THF (20 mL) and $Et_3N$ (0.2 mL). The mixture was filtered after stirring for 5 h at room temperature. Evaporation of solvent from the filtrate gave the residue, which was further purified by column chromatography on silica gel ($CH_2Cl_2$/petroleum ether) to afford **1** as a yellow solid (yield 50%). MS (EI): $m/z = 347$ ($M^+$); $^1$H NMR ($CD_3CN$, $\delta$ ppm, 400 MHz): 2.93 (s, 6H), 6.47 (s, 2H), 6.60 (s, 1H), 6.67 (d, 2H, $J = 9.0$ Hz), 7.29 (d, 2H, $J = 9.0$ Hz); $^{13}$C NMR ($CD_3COCD_3$, $\delta$ ppm): 40.1, 79.0, 96.0, 107.9, 108.5, 112.6, 113.6, 116.9, 120.3, 120.5, 124.2, 133.6, 151.8; Anal. Calcd for $C_{16}H_{13}NS_4$: C, 55.29; H, 3.77; N, 4.03. Found: C, 55.12; H, 3.76; N, 4.00.

**4-Tetrathiafulvalenylethynylmethoxybenzene (2).** Compound **2** was synthesized by a procedure similar to that for **1**, except that 4-ethynyl-1-methoxybenzene (40 mg, 0.3 mmol) was used in place

of 4-ethynyl-*N*,*N*-dimethylbenzenamine. This product was obtained as an orange-yellow solid (yield 60%), after separation by chromatography on silica gel ($CH_2Cl_2$/petroleum ether). MS (EI): $m/z$ = 334 ($M^+$); $^1$H NMR ($CD_3CN$, $\delta$ ppm, 400 MHz): 4.01 (s, 3H), 6.71 (s, 2H), 6.93 (s, 1H), 7.15 (d, 2H, $J$ = 8.0 Hz), 7.64 (d, 2H, $J$ = 8.0 Hz); $^{13}$C NMR ($CD_3COCD_3$, $\delta$ ppm): 55.8, 79.7, 94.2, 107.5, 114.0, 114.4, 115.2, 116.2, 120.3, 120.5, 125.8, 134.0, 161.5; Anal. Calcd for $C_{15}H_{10}OS_4$: C, 53.86; H, 3.01. Found: C, 53.66; H, 2.99. The crystal structure has been deposited at the Cambridge Crystallographic Data Center with the deposition number CCDC616393.

**Tetrathiafulvalenylethynyl Benzene (3).** Compound **3** was synthesized by the procedure similar to that for **1**, except that 1-ethynylbenzene (41 mg, 0.3 mmol) was used in place of 4-ethynyl-*N*,*N*-dimethylbenzenamine. This product was obtained as an orange-yellow solid (yield 87%), after separation by chromatography on silica gel ($CH_2Cl_2$/petroleum ether). MS (EI): $m/z$ = 304 ($M^+$); $^1$H NMR ($d_6$-DMSO, $\delta$ ppm, 400 MHz): 6.77 (s, 2H), 7.23 (s, 1H), 7.40−7.53 (m, 4H); $^{13}$C NMR ($CD_3COCD_3$, $\delta$ ppm): 81.0, 93.9, 107.3, 114.4, 115.8, 120.3, 120.5, 122.6, 127.0, 129.6, 130.2, 132.4; Anal. Calcd for $C_{14}H_8S_4$: C, 55.23; H, 2.65. Found: C, 55.59; H, 2.73.

**4-Tetrathiafulvalenylethynylfluorobenzene (4).** Compound **4** was synthesized by a procedure similar to that for **1**, except that 4-ethynyl-1-fluorobenzene (36 mg, 0.3 mmol) was used in place of 4-ethynyl-*N*,*N*-dimethylbenzenamine. This product was obtained as an orange-yellow solid (yield 60%), after separation by chromatography on a silica gel ($CH_2Cl_2$/petroleum ether). MS (EI): $m/z$ = 322 ($M^+$); $^1$H NMR ($CD_3CN$, $\delta$ ppm, 400 MHz): 6.71 (s, 2H), 7.00 (s, 1H), 7.36 (m, 2H), 7.73 (m, 2H); $^{13}$C NMR ($CDCl_3$, $\delta$ ppm): 85.9, 92.5, 115.7, 115.8, 116.1, 118.2, 119.0, 119.2, 124.7, 133.8, 164.3; Anal. Calcd for $C_{14}H_7FS_4$: C, 52.15; H, 2.19. Found: C, 52.17; H, 2.26.

**4-Tetrathiafulvalenylethynylnitrobenzene (5).** Compound **5** was synthesized by a procedure similar to that for **1**, except that 4-ethynyl-1-nitrobenzene (40 mg, 0.3 mmol) was used in place of 4-ethynyl-*N*,*N*-dimethylbenzenamine. This product was obtained as a black-red solid (yield 92%), after separation by chromatography on a silica gel (ethyl acetate/$CH_2Cl_2$). MS (EI): $m/z$ = 349 ($M^+$); $^1$H NMR ($CD_3CN$, $\delta$ ppm, 400 MHz): 6.51 (s, 2H), 6.94 (s, 1H), 7.68 (d, 2H, $J$ = 9.0 Hz), 8.21 (d, 2H, $J$ = 9.0 Hz); $^{13}$C NMR ($CD_3COCD_3$, $\delta$ ppm): 85.5, 92.0, 106.7, 115.0, 120.3, 120.5, 124.7, 129.3, 129.8, 133.4, 134.7, 148.6; Anal. Calcd for $C_{14}H_7NO_2S_4$: C, 48.12; H, 2.02; N, 4.01. Found: C, 48.11; H, 2.20; N, 4.02.

**2-Tetrathiafulvalenylethynylpyridine (6).** Compound **6** was synthesized by a procedure similar to that for **1**, except that 2-ethynylpyridine (26 mg, 0.3 mmol) was used in place of 4-ethynyl-*N*,*N*-dimethylbenzenamine. This product was obtained as a red solid (yield 78%), after separation by chromatography on silica gel (ethyl acetate/$CH_2Cl_2$). MS (EI): $m/z$ = 305 ($M^+$); $^1$H NMR ($CD_3CN$, $\delta$ ppm, 400 MHz): 6.51 (s, 2H), 6.95 (s, 1H), 7.37 (m, 1H), 7.54 (d, 1H, $J$ = 8.0 Hz), 7.79 (m, 1H), 8.56 (d, 1H, $J$ = 4.8 Hz); $^{13}$C NMR ($CDCl_3$, $\delta$ ppm): 80.3, 92.2, 107.9, 113.6, 115.2, 118.8, 119.1, 123.2, 127.1, 127.2, 136.3, 142.4, 150.2; Anal. Cacld for $C_{13}H_7NS_4$: C, 51.12; H, 2.31; N, 4.59. Found: C, 51.29; H, 2.41; N, 4.67.

**3-Tetrathiafulvalenylethynylpyridine (7).** Compound **7** was synthesized by a procedure similar to that for **1**, except that 3-ethynylpyridine (26 mg, 0.3 mmol) was used in place of 4-ethynyl-*N*,*N*-dimethylbenzenamine. This product was obtained as a red solid (yield 82%), after separation by chromatography on silica gel (ethyl acetate/$CH_2Cl_2$). MS (EI): $m/z$ = 305 ($M^+$); $^1$H NMR ($CD_3CN$, $\delta$ ppm, 400 MHz): 6.51 (s, 2H), 6.87 (s, 1H), 7.38 (m, 1H), 7.85 (m, 1H), 8.54 (m, 1H), 8.65 (d, 1H); $^{13}$C NMR ($CDCl_3$, $\delta$ ppm): 83.8, 89.9, 107.7, 113.8, 115.3, 118.8, 119.1, 119.3, 123.1, 126.0, 138.4, 149.1, 152.1; Anal. Calcd for $C_{13}H_7NS_4$: C, 51.12; H, 2.31; N, 4.59. Found: C, 51.14; H, 2.44; N, 4.55.

**4-Tetrathiafulvalenylethynylpyridine (8).** Compound **8** was synthesized by a procedure similar to that for **1**, except that 4-ethynylpyridine (26 mg, 0.3 mmol) was used in place of 4-ethynyl-*N*,*N*-dimethylbenzenamine. This product was obtained as a red solid (yield 75%), after separation by chromatography on silica gel (ethyl acetate/$CH_2Cl_2$). MS (EI): $m/z$ = 305 ($M^+$); $^1$H NMR ($CD_3CN$, 400 MHz) $\delta$: 6.51 (s, 2H), 6.94 (s, 1H), 7.39 (m, 2H), 8.56 (m, 2H); $^{13}$C NMR ($CDCl_3$, $\delta$ ppm): 85.0, 90.6, 107.5, 114.4, 115.2, 119.0, 119.3, 125.4, 127.4, 130.3, 150.0; Anal. Cacld for $C_{13}H_7NS_4$: C, 51.12; H, 2.31; N, 4.59. Found: C, 50.92; H, 2.40; N, 4.76.

**Binding Constant Determination.** The absorption spectral titration for the determination of binding constants was performed at 298 K. The supporting electrolyte (0.1 mol/L tetrabutylammonium hexafluorophosphate) was added to maintain a constant ionic strength of the sample solution. The ion binding constants ($K_s$) were calculated from the following equation:[17]

$$A_0/(A_0 - A) = A_0/\alpha C_0 + (A_0/\alpha C_0 K_s)(1/[M]) \quad (1)$$

where $A$ and $A_0$ are the absorbances for **6**−**8** at 422, 418, and 550 nm in the presence and absence of metal ion, respectively; $\alpha$ is the ratio of the pyridyl-substituted compound and $Pb^{2+}$; $C_0$ is the concentration of **6**−**8**; and [M] is the concentration of the $Pb^{2+}$ ion.

**Acknowledgment.** We are grateful for financial support from the National Science Foundation of China (20333080, 20332040, 20472091, 50473048, 20472092, and 20403025), the Ministry of Science and Technology of China (Grants 2003CB716802, 2004CB719903, 2006CB806105, and G2007CB808004), and the Bureau for Basic Research of the Chinese Academy of Sciences.

**Supporting Information Available:** Physical measurements, absorption spectra of **6** and **7** in $CH_3CN$ solution as a function of concentration of $Pb^{2+}$, $^1$H NMR spectra of **6** and **7** in the absence and presence of $Pb^{2+}$ in acetone-$d_6$, CV titration spectra of **6** and **7** in $CH_3CN$ with $Pb^{2+}$, and crystal structure data (CIF) of **2**. This material is available free of charge via the Internet at http://pubs.acs.org.

JO0622577